Computers & Fluids Vol. 16, No. 2, pp. 183–193, 1988
Printed in Great Britain.

0045-7930/88 $3.00 + 0.00

MAGNETOHYDRODYNAMIC FLOW AND HEAT TRANSFER ABOUT A ROTATING DISK WITH SUCTION AND INJECTION AT THE DISK SURFACE

S. KISHORE KUMAR,[1] WILLIAM I. THACKER[2] and LAYNE T. WATSON[3]

[1]Director's Unit, National Aeronautical Laboratory, Bangalore India 560 017, [2]Computer Science, Winthrop College, Rock Hill, SC 29730, U.S.A. and [3]Departments of Electrical Engineering and Computer Science, Industrial and Operations Engineering, and Mathematics, University of Michigan, Ann Arbor, MI 48109–1092, U.S.A.

(*Received* 17 *July* 1986; *in revised form* 7 *July* 1987)

Abstract—This paper studies the effects of an axial magnetic field on the flow and heat transfer about a porous rotating disk. Using modern quasi-Newton and globally convergent homotopy methods, numerical solutions are obtained for a wide range of magnetic field strengths and injection and suction velocities. Results are presented graphically in terms of three nondimensional parameters. There is excellent agreement with previous work and asymptotic formulas.

1. INTRODUCTION

Von Karman [1] first noted that the Navier–Stokes equations governing the flow past a rotating disk reduced to self similar form. He also obtained an approximate solution for that problem. Later, Cochran [2] obtained a more accurate solution to the same problem. The effects of an axial magnetic field on the flow and heat transfer about a rotating disk were studied by Sparrow and Cess [3], and asymptotic solutions for the flow were obtained by Kakutani [4]. Beginning with the pioneering work of Prandtl in 1904 on mass addition or removal at a bounding surface, there has been continuing interest due to the wide range of applications. Some important examples are boundary layer control, cooling of turbine blades, and cooling the skins of high speed aircraft. Another significant application is to model the boundary layer on the face of a crystal grown by the Czochralski method with an axial magnetic field (Hurle and Series [5]). Considerable work has been done recently on the effects of uniform suction or injection on the flow field induced by a rotating disk. Stuart [6] obtained a series solution for strong suction at the surface of a rotating disk. Sparrow and Gregg [7] developed numerical solutions for the rotating disk problem with suction or injection at the disk surface. Kuiken [8] examined the case of strong injection at the disk surface. Ackroyd [9] obtained uniformly valid series solutions for suction velocities and low values of injection velocities.

In this paper we describe the effects of an axial magnetic field and suction (or injection) on the flow and heat transfer about an insulated rotating disk. Pande [10] obtained a series solution for this problem when there is strong suction and a weak magnetic field. We will present results on the flow and heat transfer for a wider range of injection velocities and suction velocities combined with a wide range of magnetic field strengths. When the disk is conducting, adding a magnetic field promotes the motion of the fluid, whereas if the disk is insulated, adding a magnetic field decreases the flow velocities. Conducting disk problems belong to the class discussed by Lin [11], and are not considered here.

2. GOVERNING EQUATIONS AND BOUNDARY CONDITIONS

Let the disk lie in the plane $z = 0$ and the space $z \geqslant 0$ be occupied by a homogeneous, incompressible, electrically conducting viscous fluid. The geometry of the problem being studied is shown in Fig. 1. Here (r, θ, z) are cylindrical coordinates, B_0 is the externally applied magnetic field in the z direction, ω is the angular velocity of the disk, T_w is the uniform temperature at the disk surface and T_∞ is the ambient fluid temperature. the basic

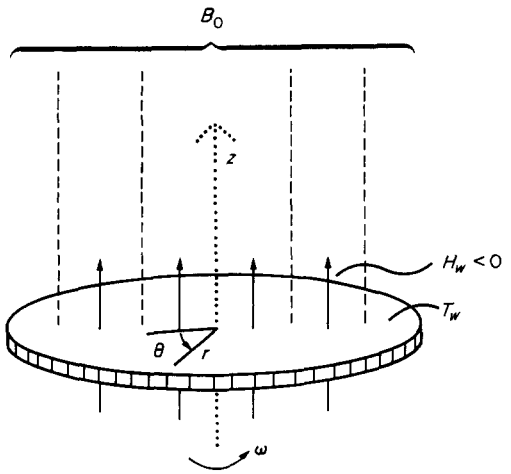

Fig. 1. Coordinate system.

equations for a nonconducting disk are modified to include the Lorenz force $\vec{J} \times \vec{B}$ ($\vec{J}$ being the current density).

In cylindrical coordinates (r, θ, z), assuming angular symmetry, the equations of motion are [3]:

$$\rho\left[\left(u\frac{\partial}{\partial r}+w\frac{\partial}{\partial z}\right)u-\frac{v^2}{r}\right]=-\frac{\partial p}{\partial r}+\mu\left(\nabla^2 u-\frac{u}{r^2}\right)-\sigma u B_0^2, \tag{1}$$

$$\rho\left[\left(u\frac{\partial}{\partial r}+w\frac{\partial}{\partial z}\right)v+\frac{uv}{r}\right]=\mu\left(\nabla^2 v-\frac{v}{r^2}\right)-\sigma v B_0^2, \tag{2}$$

$$\rho\left[u\frac{\partial}{\partial r}+w\frac{\partial}{\partial z}\right]w=-\frac{\partial p}{\partial z}+\mu\nabla^2 w, \tag{3}$$

and the continuity equation is

$$\frac{\partial}{\partial r}(ru)+\frac{\partial}{\partial z}(rw)=0, \tag{4}$$

where u, v and w are the velocity components in the r, θ, z directions respectively, ρ is the density of the fluid, μ is the coefficient of viscosity, p is the pressure, σ is the electrical conductivity and:

$$\nabla^2=\frac{\partial^2}{\partial r^2}+\frac{1}{r}\frac{\partial}{\partial r}+\frac{\partial^2}{\partial z^2}.$$

Further, equations (1)–(3) assume that the induced electric field is negligible compared with the imposed magnetic field. This assumption is valid for flow at low magnetic Prandtl number as shown by Rossow [12] and Neuringer and McIlroy [13]. The energy equation is:

$$\left(u\frac{\partial}{\partial r}+w\frac{\partial}{\partial z}\right)T=\alpha\nabla^2 T, \tag{5}$$

in which T is the static temperature and α is the thermal diffusivity. The boundary conditions of the problem are:

$$\left.\begin{aligned} u&=0\\ v&=r\omega\\ w&=-H_w\\ T&=T_w \end{aligned}\right\} \quad \text{at} \quad z=0, \qquad \left.\begin{aligned} u&\to 0\\ v&\to 0\\ T&\to T_\infty \end{aligned}\right\} \quad \text{as} \quad z\to\infty, \tag{6}$$

where $H_w > 0$ corresponds to suction and $H_w < 0$ corresponds to injection.

3. REDUCTION TO ORDINARY DIFFERENTIAL EQUATIONS

Following Von Karman [1], we introduce the following relations:

$$u = r\omega F(\eta), \qquad v = r\omega G(\eta), \qquad w = (\omega\upsilon)^{1/2} H(\eta),$$

$$P(\eta) = \frac{p}{\mu\omega}, \qquad \Theta(\eta) = \frac{T - T_\infty}{T_w - T_\infty}, \qquad \eta = z\left(\frac{\omega}{\upsilon}\right)^{1/2}. \tag{7}$$

Also, from equation (4) we have:

$$F(\eta) = -\frac{H'(\eta)}{2}. \tag{8}$$

Substituting equations (7) and (8) into equations (1)–(5) yields:

$$H''' = HH'' - \frac{(H')^2}{2} + mH' + 2G^2, \tag{9a}$$

$$G'' = HG' - H'G + mG, \tag{9b}$$

$$\Theta'' = Pr H\Theta', \tag{10}$$

where prime denotes differentiation with respect to η. The Prandtl number Pr and the magnetic parameter m are given by:

$$\mathrm{Pr} = \frac{\upsilon}{\alpha}, \quad m = \frac{\sigma B_0^2}{\rho\omega}, \tag{11}$$

where $\upsilon = \mu/\rho$ is the kinematic coefficient of viscosity. In terms of the new variables defined in equation (7), the new boundary conditions from equation (6) are:

$$\left.\begin{aligned} H' &= 0 \\ H &= -A \\ G &= 1 \\ \Theta &= 1 \end{aligned}\right\} \text{ at } \eta = 0, \qquad \left.\begin{aligned} H' &\to 0 \\ G &\to 0 \\ \Theta &\to 0 \end{aligned}\right\} \text{ as } \eta \to \infty, \tag{12}$$

where A is the nondimensional velocity normal to the disk surface. $A > 0$ represents suction while $A < 0$ represents injection. Observe that equation (10) decouples from equations (9a) and (9b), and that once $H(\eta)$ has been determined, $\Theta(\eta)$ can be computed by solving a relatively easy 1-D two-point boundary value problem.

4. NUMERICAL METHOD

Following the format in Heruska [14], define:

$$X = \begin{pmatrix} H''(0) \\ G'(0) \end{pmatrix}. \tag{13}$$

Let $H(\eta; X)$, $G(\eta; X)$ be the solution of the initial value problem given by equation (9) with the initial conditions (12) and (13). The original two point boundary value problem described by equations (9) and (12) is numerically equivalent to solving the nonlinear system of equations:

$$F(X) = \begin{pmatrix} H'(\tau; X) \\ G(\tau; X) \end{pmatrix} = 0, \tag{14}$$

where τ is chosen large enough so that $|H(\eta) - H(\tau)| < \epsilon$ and $|G(\eta) - G(\tau)| < \epsilon$ for $\tau < \eta < \infty$ and a given $\epsilon > 0$. Equation (14) is derived from the boundary conditions (12). Algorithms for solving nonlinear systems like (14) typically require partial derivatives such as $\partial H'/\partial X_k$. We can write the functions needed as:

$$Y = \left(H(\eta), H'(\eta), H''(\eta), G(\eta), G'(\eta), \frac{\partial H(\eta)}{\partial X_k}, \frac{\partial H'(\eta)}{\partial X_k}, \frac{\partial H''(\eta)}{\partial X_k}, \frac{\partial G(\eta)}{\partial X_k}, \frac{\partial G'(\eta)}{\partial X_k}\right),$$

for $k = 1$ and $k = 2$. Now $H'(\eta; X)$, $G(\eta; X)$ and their partial derivatives can be calculated from the first order system:

$$\begin{aligned}
Y_1' &= Y_2 \\
Y_2' &= Y_3 \\
Y_3' &= Y_1 Y_3 - \frac{Y_2^2}{2} + mY_2 + 2Y_4^2 \\
Y_4' &= Y_5 \\
Y_5' &= Y_1 Y_5 - Y_2 Y_4 + mY_4 \\
Y_6' &= Y_7 \\
Y_7' &= Y_8 \\
Y_8' &= Y_1 Y_8 + Y_6 Y_3 - Y_2 Y_7 + 4Y_9 Y_4 + mY_7 \\
Y_9' &= Y_{10} \\
Y_{10}' &= Y_1 Y_{10} + Y_6 Y_5 - Y_7 Y_4 - Y_9 Y_2 + mY_9
\end{aligned} \tag{15a}$$

$$Y(0) = (-A, 0, X_1, 1, X_2, 0, 0, \delta_{1k}, 0, \delta_{2k}) \tag{15b}$$

where δ_{ik} is the Kronecker delta. By solving this system twice, for $k = 1$ and $k = 2$, the Jacobian matrix $DF(X)$ of $F(X)$ can be calculated.

Two methods were utilized to solve this problem, a quasi-Newton method and a globally convergent homotopy method. The quasi-Newton method used was HYBRJ from the MINPACK subroutine package by Argonne National Laboratory [15]. These quasi-Newton routines are robust and quite efficient. However, they fail at times by converging to local minima.

The other method, a globally convergent homotopy method developed by Watson [16], does not suffer from the convergence problems of the quasi-Newton method. However, this method requires considerably more computation time. Details about the algorithm and some of its applications can be found in [16–19].

The strategy for these problems was to try to solve them first using the inexpensive quasi-Newton method. If that fails, then use the expensive, but guaranteed convergent, homotopy algorithm.

As previously mentioned, these methods use some partial derivatives with respect to the initial conditions. For some values of m and A, these partials increase drastically as η increases. This problem was worse in cases where m was large and/or there was large injection velocity. Large values of suction velocity tended to make the problem better conditioned. Therefore, results with large m and/or large injection velocities are not as accurate as other results. This also limited the range of injection velocities and m values for which solutions could be computed. Such instability is an inherent problem with shooting methods, the type used. Other methods, such as finite difference, collocation, and finite element, will be considered in future work.

5. DISCUSSION

The flow depends on two parameters, A and m, while the temperature depends on Pr, A and m. Graphs are presented to gain some insight into the effects of these parameters. For $m = 0$ we have the case of a rotating disk in the absence of a magnetic field while $A = 0$ corresponds to the case of an impermeable rotating disk. The effects of A and m on radial velocity ($F(\eta)$) are shown in Fig. 2. From these figures, we see that the radial velocity increases monotonically with increased η, until a maximum is reached, and then decreases monotonically to 0 as $\eta \to \infty$. For an imposed magnetic field, as the value of suction decreases (Fig. 2a), the maximum for radial velocity moves away from the disk and the magnitude of the radial velocity increases. Increasing the value for injection moves the maximum away from the disk and increases the maximum radial velocity. For an imposed

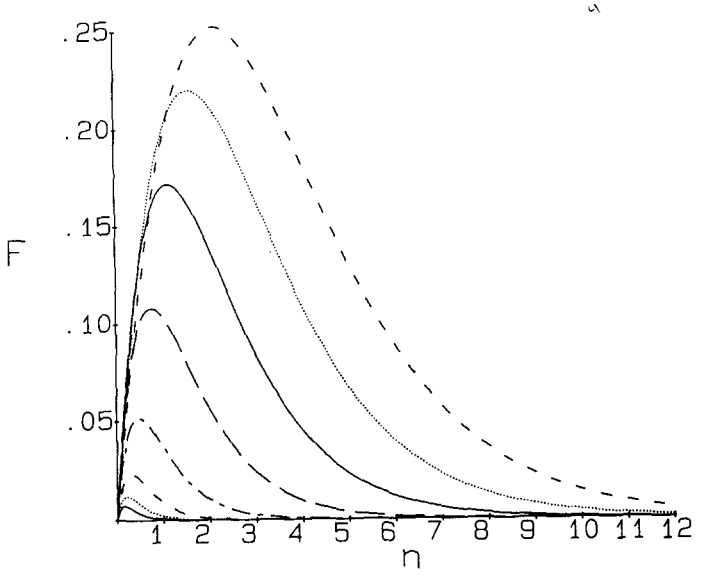

(a)

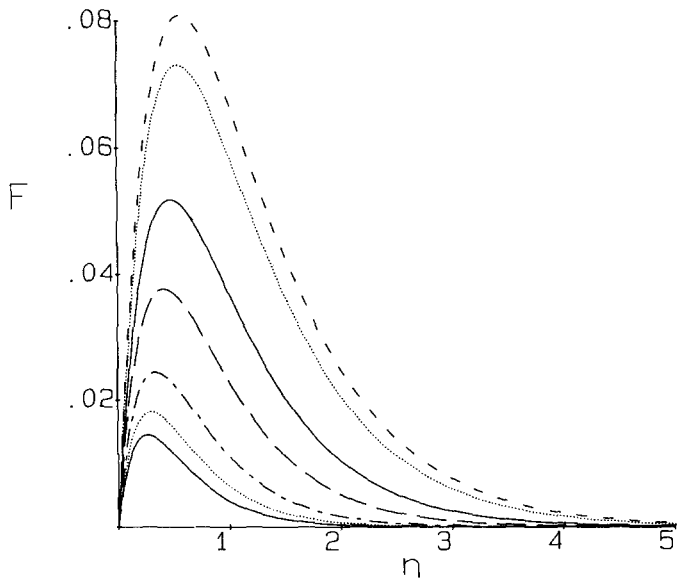

(b)

Fig. 2. Radial velocity F. (a) Effect of A, $m = 0.5$, $A = -3.0, -2.0, -1.0, 0.0, 1.0, 2.0, 3.0, 4.0$ (top to bottom). (b) Effect of m, $A = 1.0$, $m = 0.0, 0.1, 0.5, 1.0, 2.0, 3.0, 4.0$ (top to bottom).

suction value, as the strength of the magnetic field increases (Fig. 2b), the maximum radial velocity moves towards the disk and the magnitude of this maximum decreases. From these two figures, it can be inferred that for large values of m, there is a considerable reduction in the 3-D character of radial velocity (i.e. the flow becomes 2-D).

Figure 3 shows the behavior of the tangential velocity ($G(\eta)$) for various values of A and m. For an imposed magnetic field, as suction increases (Fig. 3a), the boundary layer thickness increases, whereas an opposite effect is observed for increasing injection values. Figures 3(b) and (c) show the effects of various magnetic fields on the tangential velocity for $A = 1.0$ and -1.0. In both cases an increase in magnetic field has the same effect as that of increasing suction, namely thinning of the boundary layer.

Figure 4(a) shows that with an imposed magnetic field, for higher values of suction the axial velocity is almost constant with respect to η. When A is -1.0, there is still some inflow

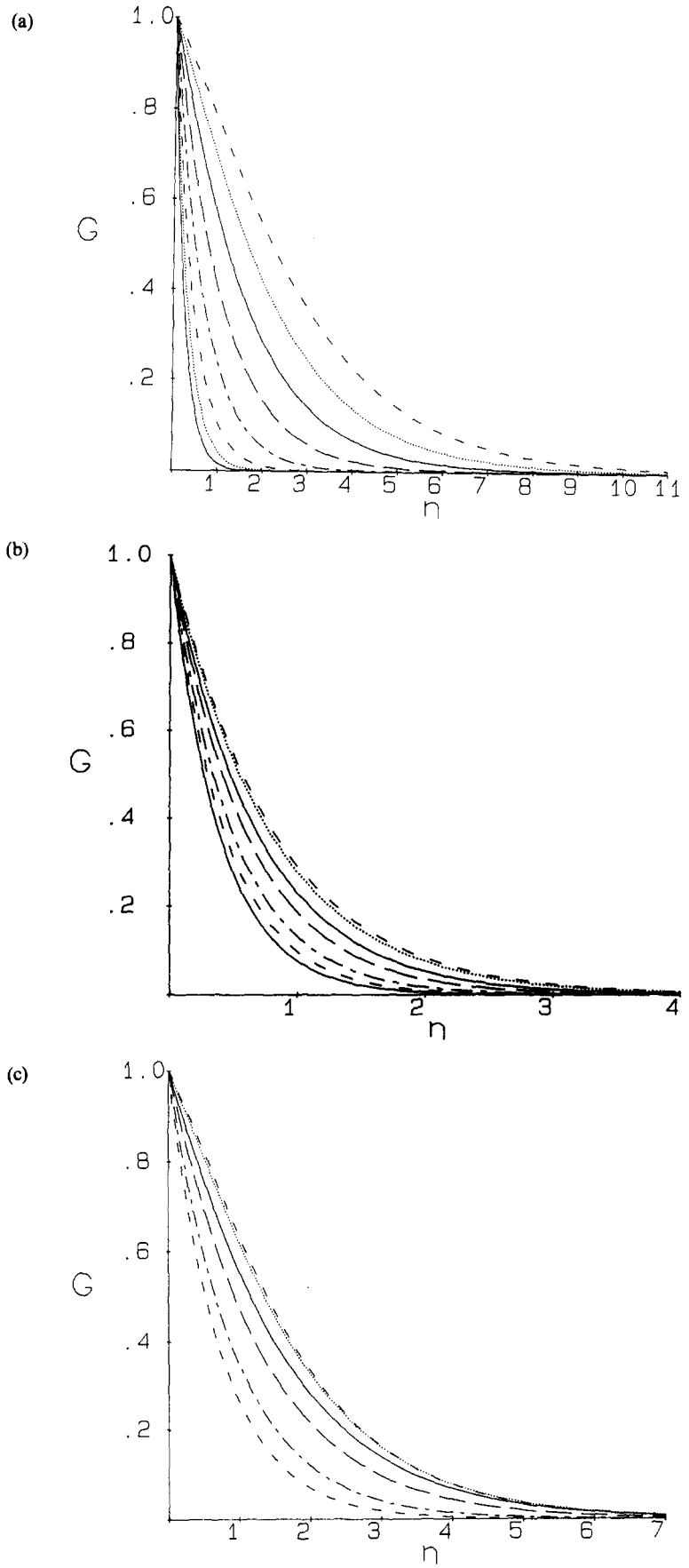

Fig. 3. Tangential velocity G. (a) Effect of A, $m = 0.5$, $A = -3.0, -2.0, -1.0, 0.0, 1.0, 2.0, 3.0, 4.0$ (top to bottom). (b) Effect of m with suction, $A = 1.0$, $m = 0.0, 0.1, 0.5, 1.0, 2.0, 3.0, 4.0$ (top to bottom. (c) Effect of m with injection, $A = -1.0$, $m = 0.0, 0.1, 0.5, 1.0, 2.0, 3.0$ (top to bottom).

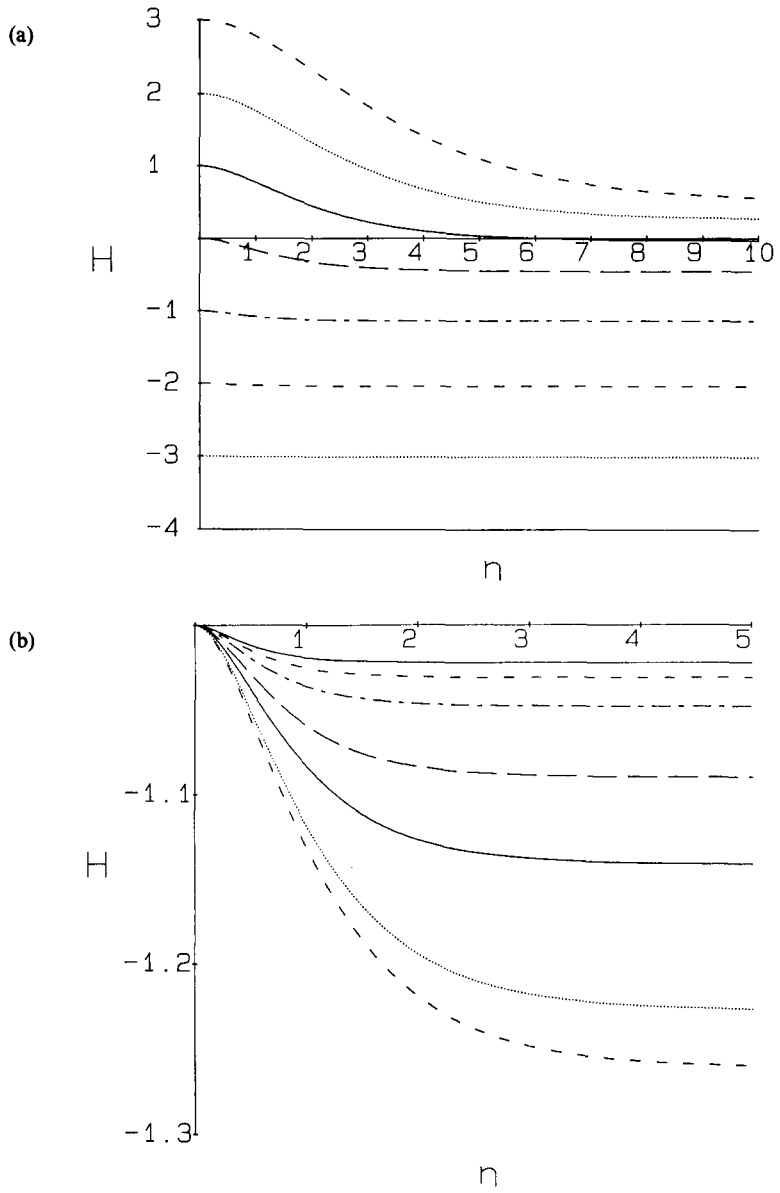

Fig. 4. Axial velocity H. (a) Effect of A, $m = 0.5$, $A = -3.0, -2.0, -1.0, 0.0, 1.0, 2.0, 3.0, 4.0$ (top to bottom). (b) Effect of m, $A = 1.0$, $m = 4.0, 3.0, 2.0, 1.0, 0.5, 0.1, 0.0$ (top to bottom).

in the axial direction at infinity. But, as the injection value increase $(-2, -3)$, there is no inflow at all. We can understand this better by referring to Table 1. For $m = 0.1$ there is inflow towards the disk in the axial direction from infinity ($H(\infty)$ is negative) for all values of injection. For $m = 0.5$ there is no inflow from infinity ($H(\infty)$ is positive) when the injection value has a larger magnitude than -2.0. The effect of m on H can be seen from Fig. 8 and Table 1. For small values of suction, as the strength of the magnetic field increases, the axial flow towards the disk decreases. For larger values of suction ($A > 2.0$), the increase in magnetic field has less effect on $H(\infty)$. For small injection values ($A = -0.1$), $H(\infty)$ becomes positive when $m = 4.0$; for $A = -0.5$ onwards, $H(\infty)$ becomes positive for smaller values of m.

The torque (M) required to overcome the shear on one side of the disk is given by:

$$\frac{2M}{\pi r_0^4 \rho (\upsilon \omega^3)^{1/2}} = -G'(0), \tag{16}$$

Table 1. Effect of A and m on torque ($G'(0)$), axial velocity at infinity ($H(\infty)$), displacement thickness (δ^*) and momentum thickness ($\delta_\dagger^*$)

A	m	$H''(0)$	$G'(0)$	$H(\infty)$	$\delta^*(\omega/\upsilon)^{1/2}$	$\delta_\dagger^*(\omega/\upsilon)^{1/2}$
0.1	0.1	−0.94970031	−0.70556753	−0.80728	1.1888	0.56923
0.1	0.5	−0.75941834	−0.89547865	−0.51409	1.0308	0.50523
0.1	1.0	−0.61001359	−1.1179265	−0.33015	0.86351	0.42797
0.1	2.0	−0.45588843	−1.4921873	−0.20045	0.66254	0.33033
0.1	4.0	−0.32862435	−2.0606763	−0.13849	0.48375	0.24168
0.5	0.1	−0.87549736	−0.90682387	−0.95198	1.0012	0.48878
0.5	0.5	−0.69933108	−1.1086137	−0.76389	0.86247	0.42644
0.5	1.0	−0.56725454	−1.3356967	−0.65346	0.73299	0.36456
0.5	2.0	−0.43130013	−1.7095775	−0.57285	0.58047	0.28968
0.5	4.0	−0.31608844	−2.2746559	−0.53043	0.43859	0.21917
1.0	0.1	−0.73348580	−1.2305623	−1.2269	0.78192	0.38723
1.0	0.5	−0.60106000	−1.4357645	−1.1410	0.68282	0.33973
1.0	1.0	−0.50208794	−1.6570758	−1.0898	0.59708	0.29775
1.0	2.0	−0.39513646	−2.0184735	−1.0481	0.49318	0.24631
1.0	4.0	−0.29803228	−2.5693250	−1.0225	0.38858	0.19421
2.0	0.1	−0.46957149	−2.0834812	−2.0536	0.47727	0.23830
2.0	0.5	−0.42074136	−2.2490111	−2.0413	0.44289	0.22123
2.0	1.0	−0.37743805	−2.4313615	−2.0318	0.41017	0.20494
2.0	2.0	−0.32102279	−2.7423451	−2.0213	0.36407	0.18197
2.0	4.0	−0.25887694	−3.2413392	−2.0123	0.30828	0.15411
3.0	0.1	−0.32592346	−3.0445028	−3.0175	0.32804	0.16397
3.0	0.5	−0.30740555	−3.1678635	−3.0153	0.31534	0.15763
3.0	1.0	−0.28844315	−3.3105664	−3.0131	0.30180	0.15087
3.0	2.0	−0.25964084	−3.5671320	−3.0102	0.28017	0.14006
3.0	4.0	−0.22194538	−4.0034081	−3.0069	0.24970	0.12484
4.0	0.1	−0.24719169	−4.0298749	−4.0076	0.24804	0.12401
4.0	0.5	−0.23870361	−4.1258146	−4.0070	0.24229	0.12113
4.0	1.0	−0.22932912	−4.2400206	−4.0064	0.23577	0.11788
4.0	2.0	−0.21370296	−4.4526459	−4.0054	0.22452	0.11226
4.0	4.0	−0.19061247	−4.8306252	−4.0041	0.20698	0.10348
5.0	0.1	−0.19864430	−5.0225310	−5.0039	0.19907	0.099530
5.0	0.5	−0.19413489	−5.1005006	−5.0037	0.19603	0.098010
5.0	1.0	−0.18894688	−5.1948049	−5.0035	0.19247	0.096232
5.0	2.0	−0.17980709	−5.3741780	−5.0031	0.18605	0.093023
5.0	4.0	−0.16516062	−5.7030098	−5.0025	0.17533	0.087663
0.0	0.1	−0.96096043	−0.66211964	−0.77929	1.2363	0.58847
0.0	0.5	−0.77026519	−0.84872385	−0.45888	1.0755	0.52567
0.0	1.0	−0.61851596	−1.0690534	−0.25331	0.89896	0.44505
0.0	2.0	−0.46111824	−1.4420940	−0.10858	0.68477	0.34131
0.0	4.0	−0.33140610	−2.0102667	−0.040775	0.49577	0.24767
−0.1	0.1	−0.96927842	−0.62109785	−0.75394	1.2839	0.60729
−0.1	0.5	−0.77923730	−0.80441572	−0.40639	1.1210	0.54628
−0.1	1.0	−0.62598320	−1.0223583	−0.17809	0.93547	0.46256
−0.1	2.0	−0.46591593	−1.3937003	−0.017229	0.70768	0.35262
−0.1	4.0	−0.33402817	−1.9610945	0.056832	0.50807	0.25381
−0.5	0.1	−0.97523069	−0.47860730	−0.67365	1.4764	0.67862
−0.5	0.5	−0.79618949	−0.64963677	−0.22074	1.3106	0.62967
−0.5	1.0	−0.64470132	−0.85634630	0.10702	1.0912	0.53644
−0.5	2.0	−0.48031949	−1.2168142	0.34294	0.80587	0.40097
−0.5	4.0	−0.34276608	−1.7766978	0.44613	0.56019	0.27976
−1.0	0.1	−0.93342121	−0.34145130	−0.60563	1.7252	0.76046
−1.0	0.5	−0.77949348	−0.49935791	−0.032133	1.5623	0.73459
−1.0	1.0	−0.64332440	−0.69066292	0.43166	1.3048	0.63569
−1.0	2.0	−0.40244571	−1.3204110	0.78156	0.94240	0.46784
−1.0	4.0	−0.34935998	−1.5731223	0.93015	0.63162	0.31531
−2.0	0.1	−0.76986197	−0.17012160	−0.52194	2.2707	0.91238
−2.0	0.5	−0.67355551	−0.30469715	0.25947	2.1129	0.94692
−2.0	1.0	−0.58296165	−0.46571471	1.0075	1.7822	0.85028
−2.0	2.0	−0.46608986	−0.75841319	1.6265	1.2534	0.61869
−2.0	4.0	−0.34797800	−1.2471552	1.8900	0.79339	0.39564
−3.0	0.1	−0.60318822	−0.08888757	−0.46554	2.8897	1.0652
−3.0	0.5	−0.54997174	−0.20059342	0.49926	2.7237	1.1693
−3.0	1.0	−0.49679764	−0.33393640	1.5417	2.3084	1.0790
−3.0	2.0	−0.42062178	−0.58053840	2.4462	1.5974	0.78175
−3.0	4.0	−0.33145553	−1.0093864	2.8415	0.97518	0.48542
−4.0	0.1	−0.47811827	−0.05236093	−0.41853	3.5666	1.2289
−4.0	0.5	−0.44915707	−0.14412499	0.74209	3.3743	1.3991
−4.0	1.0	−0.41848145	−0.25452370	2.1621	2.7973	1.2495
−4.0	2.0	−0.37057638	−0.46234394	3.2866	1.9269	0.91705
−4.0	4.0	−0.30710176	−0.83580028	3.7894	1.1667	0.57715

where r_0 is the radius of the disk. The effect of m and A on $G'(0)$ can be observed from Table 1. The torque on the disk increases with m for all values of A. However, when suction is small, say $A = 0.1$, $G'(0)$ increases by nearly 192% as m increases from 0.1 to 4.0. Contrast this with the case $A = 5.0$, where the increase is only 13.5% as m increases from

0.1 to 4.0. This shows that while the effect of m on torque is large when suction is small, the effect is reduced as suction increases. Table 1 also shows that as the values for injection increase in magnitude, the effect of m on torque becomes increasingly dominant.

Under the assumptions discussed in Section 2, the current density:

$$\vec{J} = \sigma \begin{pmatrix} u \\ v \\ w \end{pmatrix} \times \vec{B} = \sigma r \omega B_0 \begin{pmatrix} G(\eta) \\ -F(\eta) \\ 0 \end{pmatrix}.$$

Using $F(\eta)$ and $G(\eta)$ computed from the initial conditions given in Table 1 or read from Figs 2 and 3, one can easily compute the current lines, which are spirals of the form:

$$r = \kappa \exp\left(-G(\eta)\theta/F(\eta)\right),$$

in the z = constant planes. The equipotential surfaces can be computed from the above expression for the current density $\vec{J}$ in terms of $F(\eta)$ and $G(\eta)$.

6. DISPLACEMENT THICKNESS AND MOMENTUM THICKNESS

For the tangential direction, define the displacement thickness δ^* as:

$$\delta^* \left(\frac{\omega}{\upsilon}\right)^{1/2} = \int_0^\infty G(\eta)\, d\eta. \tag{17}$$

The momentum thickness for the flow about a rotating disk as defined by Stuart [6] is:

$$\delta_1^* \left(\frac{\omega}{\upsilon}\right)^{1/2} = \int_0^\infty G(\eta)(1 - G(\eta))\, d\eta. \tag{18}$$

The values obtained for δ^* and δ_1^* are shown in Table 1 as functions of m and A. The displacement thickness decreases for increased suction and increases for increased injection. The displacement thickness is greatly affected by increasing m when the suction value is small, whereas the displacement thickness changes only slightly with increases in m when the suction values get larger. However, for all values of injection, displacement thickness decreases significantly with increased m. Similar trends are observed for momentum thickness.

7. HEAT TRANSFER

From Fourier's Law, the heat transfer from the disk to the fluid in transformed variables is

$$q = -\kappa(T_w - T_\infty)\left(\frac{\omega}{\upsilon}\right)^{1/2} \Theta'(0), \tag{19}$$

where κ is the thermal conductivity. The Nusselt number is given by:

$$\mathrm{Nu} = \frac{q(\upsilon/\omega)^{1/2}}{(T_w - T_\infty)\kappa}. \tag{20}$$

From equations (19) and (20):

$$\mathrm{Nu} = -\Theta'(0). \tag{21}$$

An expression for $-\Theta'(0)$ is obtained by integrating equation (10) subject to the boundary conditions (12) resulting in:

$$-\Theta'(0) = \frac{1}{\displaystyle\int_0^\infty \exp\left[\mathrm{Pr}\int_0^\xi H(\eta)\, d\eta\right] d\xi}. \tag{22}$$

Table 2. Effect of Prandtl number (Pr) and A on Nusselt number Nu $= -\Theta'(0)$ when $m = 0.5$

A\Pr	0.01	0.10	1.0	10.0
4.0	0.040069	0.4006091	4.002395	40.00112
3.0	0.030151	0.3013329	3.005322	30.00255
2.0	0.024076	0.2036261	2.015051	20.00770
1.0	0.011394	0.1126061	1.059119	10.03991
0.0	0.004556	0.0428310	0.2826559	0.9515366
−1.0	0.000318	0.0031799	0.0034330	

Table 3. Effect of m and Pr on Nu when $A = 1.0$

m\Pr	0.01	0.10	1.0	10.0
0.0	0.012566	0.1225589	1.0925388	10.054518
0.5	0.011394	0.1126061	1.0591194	10.039911
1.0	0.010889	0.1081711	1.0418339	10.031811
2.0	0.010477	0.1044617	1.0254037	10.023168
3.0	0.010311	0.1029297	1.0177857	10.018525
4.0	0.010224	0.1021232	1.0134742	10.015565

Table 4. Comparison of the analytic solution of Pande [10][a] and the present numerical results[b] (comparison valid only for large suction (A) and small m). $m = 0.1$

A	$-H(\infty)^a$	$-H(\infty)^b$
2.0	2.0533	2.0536
3.0	3.0175	3.0175
4.0	4.0076	4.0076
5.0	5.0039	5.0039

Some values of $-\Theta'(0)$ obtained from the above integration are shown in Tables 2 and 3. We can see that the Nusselt number $(-\Theta'(0))$ increases as suction increases but decreases as injection increases. For a given A, Nu increases as Pr increases. From Table 3, we can see that for $A = 1.0$, an increase in m from 0 to 4.0 decreases Nu by less than 19% for Pr = 0.01 and by less than 0.4% for Pr = 10.0.

Values can not be obtained for Nu with A and m parameters that result in a $H(\infty)$ value greater than 0. $H(\infty) > 0$ corresponds to fluid outflow at infinity, which makes T_∞ flow dependent. This violates the tacit assumption made in writing $\Theta(\eta)$ in equation (7). Mathematically, $H(\infty) > 0$ causes the integral in equation (22) to be unbounded and equations (10) and (12) to not have a solution.

Tables 4 and 5 show good agreement of our results with the analytical solution obtained by Pande [10] for large A and small m and the numerical results of Sparrow and Gregg [7] for $m = 0$.

8. ASYMPTOTIC COMPARISONS

Applying standard perturbation techniques to equation (9) for small A and large m yields the asymptotic formulas:

$$H = \frac{2}{3m^{3/2}}\left[\exp(-\sqrt{m}\eta) - \tfrac{1}{2}\exp(-2\sqrt{m}\eta) - \tfrac{1}{2}\right] - A, \tag{23}$$

$$-H(\infty) = \frac{1}{3m^{3/2}} + A. \tag{24}$$

From Table 6, we see that the asymptotic formula for $H(\infty)$ is fairly accurate for m values as low as 2. Also, as A increases, the percent difference decreases even though the absolute difference increases. However, negative values of A have a larger difference as well as a larger percent difference as the magnitude increases. The asymptotic formula does not have as much accuracy with injection values as it does for suction.

Table 5. Comparison of [a]the numerical solutions from Sparrow and Gregg [7] and [b]the present numerical results

A	$-H''(0)^a$	$-H''(0)^b$	$-G'(0)^a$	$-G'(0)^b$
4.0	0.2495	0.249475	4.005	4.00518
2.0	0.4848	0.484832	2.039	2.03853
0.0	1.020	1.02047	0.6159	0.615922
−1.0	0.9790	0.978962	0.3022	0.302173
−5.0	0.395	0.395131	0.0155	0.015471

Table 6. Comparison of obtained values with asymptotic formula values

A	m	$-H(\infty)_{obt}$	$-H(\infty)_{asy}$	|dif|	%|dif|
0.0	1.0	0.25331	0.33333	0.08002	24.0
0.0	2.0	0.10858	0.11785	0.00927	7.8
0.0	4.0	0.04078	0.04172	0.00094	2.3
1.0	1.0	1.0898	1.3333	0.2435	18.3
1,0	2.0	1.0481	1.1178	0.0697	6.2
1.0	4.0	1.0225	1.0417	0.0192	1.8
2.0	1.0	2.0318	2.3333	0.3015	12.9
2.0	2.0	2.0213	2.1178	0.0965	4.6
2.0	4.0	2.0123	2.0417	0.0294	1.4
3.0	1.0	3.0131	3.3333	0.3202	9.6
3.0	2.0	3.0102	3.1178	0.1076	3.5
3.0	4.0	3.0069	3.0417	0.0348	1.1
−1.0	1.0	−0.43166	−0.6667	0.23504	35.3
−1.0	2.0	−0.78157	−0.8822	0.10063	11.4
−1.0	4.0	−0.93015	−0.9583	0.02815	2.9
−2.0	1.0	−1.0070	−1.6667	0.6597	39.6
−2.0	2.0	−1.6265	−1.8822	0.2557	13.6
−2.0	4.0	−1.8900	−1.9583	0.0683	3.5
−3.0	1.0	−1.5417	−2.6667	1.1250	42.2
−3.0	2.0	−2.4462	−2.8822	0.4360	15.1
−3.0	4.0	−2.8415	−2.9583	0.1168	3.9

Acknowledgements—The work of S.K.K. was supported by a fellowship from CSIR, Delhi and the work of L.T.W. was supported by Air Force Office of Scientific Research Grant 85-0250.

REFERENCES

1. T. Von Karman, Uber laminare und turbulente reibung. *ZAMM* **1,** 233–252 (1921).
2. W. G. Cochran, The flow due to a rotating disk. *Proc. Camb. phil. Soc.* **30,** 365–375 (1934).
3. E. M. Sparrow and R. D. Cess, Magnetohydrodynamic and heat transfer about a rotating disk. *J. appl. Mech.* **29,** 181–187 (1962).
4. T. Kakutani, Hydromagnetic flow due to a rotating disk. *J. Phys. Soc. Jap.* **17,** 1496–1506 (1962).
5. D. T. J. Hurle and R. W. Series, Effective distribution coefficient in magnetic Czochralski growth. *J. Cryst. Growth* **73,** 1–9 (1985).
6. J. T. Stuart, On the effects of uniform suction on the steady flow due to a rotating disk. *Q. Jl Mech. appl. Math.* **7,** 446–457 (1954).
7. E. M. Sparrow and J. L. Gregg, Mass transfer and heat transfer about a rotating disk. *ASME J. Heat Trans.* **81,** 294–302 (1959).
8. H. K. Kuiken, The effect of normal blowing on the flow near a rotating disk of infinite extent. *J. Fluid Mech.* **47,** 789–798 (1971).
9. J. A. D. Ackroyd, On the steady flow produced by a rotating disk with either surface suction or injection. *J. Engng Math* **12,** 207–209 (1978).
10. G. S. Pande, On the effects of uniform high suction on the steady MDH flow due to a rotating disk. *Appl. Sci. Res.* **11,** 205–212 (1972).
11. C. C. Lin, Note on a class of exact solutions in magnetohydrodynamics. *Archs ration. Mech. Analysis* **1,** 1–11 (1957).
12. V. J. Rossow, Magnetohydrodynamic analysis of heat transfer near a stagnation point. *J. Aero. Sci.* **25,** 25–34 (1958).
13. J. L. Neuringer and W. McIlroy, Incompressible two dimensional stagnation point flow of an electrically conducting fluid in the presence of a magnetic field. *J. Aero Sci.* **25,** 194–203 (1958).
14. M. W. Heruska, Micropolar flow past a porous stretching sheet. *M.S. Thesis,* Dept of Computer Science, Virginia Polytechnic Institute and State University (1984).
15. J. J. Moré, B. S. Garbow and K. E. Hillstrom, User guide for MINPACK-1. ANL-80-74, Argonne National Laboratory (1980).
16. L. T. Watson, A globally convergent algorithm for computing fixed points of C^2 maps. *Appl. Math. Comput.* **5,** 297–311 (1979).
17. L. T. Watson, Numerical study of porous channel flow in a rotating system by a homotopy method. *J. Comput. appl. Math.* **7,** 21–26 (1981).
18. L. T. Watson and D. Fenner, Chow–Yorke algorithm for fixed points or zeros of C^2 maps. *ACM Trans. Math. Software* **6,** 252–259 (1980).
19. L. T. Watson, Engineering applications of the Chow–Yorke algorithm. *Appl. Math. Comput.* **9,** 111–133 (1981).